Overview of KSTAR

S. W. Yoon[a], J. G. Kwak[a], W. C. Kim[a], W. H. Ko[a], M. J. Choi[a], H. S. Hahn[a], J. Lee[a], B. H. Park[a], H. H. Lee[a], Y. In[b], H. Park[b], Y. S. Na[c], and the KSTAR Team[a]

[a] National Fusion Research Institute, Daejeon, Republic of Korea
[b] Ulsan National Institute of Science and Technology, Ulsan, Republic of Korea
[c] Seoul National University, Seoul, Republic of Korea

KSTAR

KFE 한국핵융합에너지연구원 KOREA INSTITUTE OF FUSION ENERGY

Strong contributions from domestic and international collaborators

International Collaborators

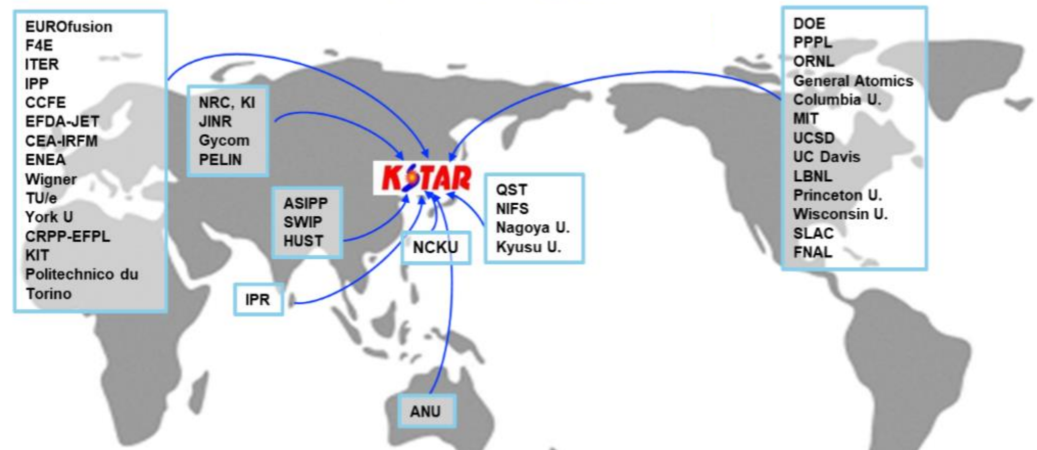

EU & Russia :

- Heating & CD (CEA)
- Diagnostics (ENEA, TU/e, Wigner)
- PWI, fueling (ITER, PELIN)
- Theory & analysis (York U)
- Experiments (JET, AUP, WEST)
- ELM, PSI, CODAC (ITER)
- ETC

Asia & Australia :

- Heating & CD (QST)
- Diagnostics (NIFS, QST, Nagoya U, Kyushu U. ASIPP, HUST, ANU)
- PWI, fueling (ASIPP, SWIP)
- MHD physics & simulation (NCKU)
- Joint workshop (A3 project)
- ETC

USA :

- Heating & CD (PPPL, GA, SLAC)
- Diagnostics (ORNL, MIT)
- 3D physics (GA, PPPL, Columbia U)
- Plasma control & CODAC (GA, PPPL, ORNL, FNAL)
- ETC

Domestic Collaborators

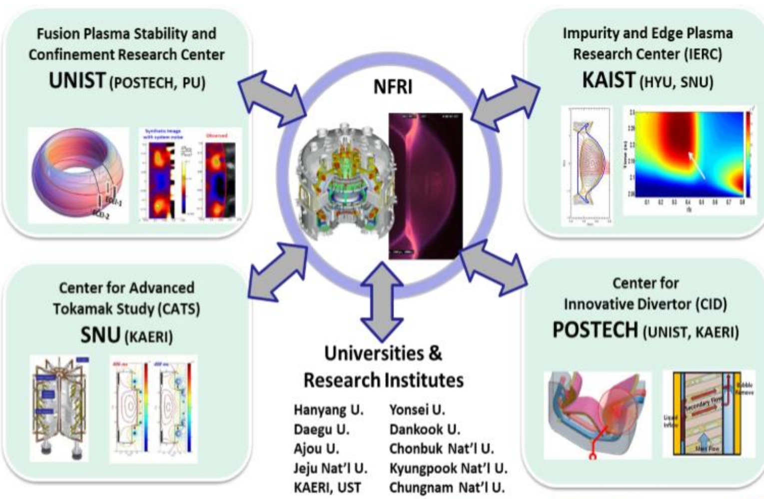

OUTLINE

- Scenario development toward high beta steady-state operation
  - Improved scenario control and extended operation windows at KSTAR
  - Further development for advanced scenario *(High q_{min}, Hybrid, high-Ti)*

- 3D field physics
  - Optimal configuration of Resonant magnetic perturbation (RMP) ELM suppression
  - Validation of the plasma response and adaptive ELM control

- Fundamental turbulence and transport
  - Interaction of MHD & turbulence in transport
  - Turbulence spreading around magnetic island and avalanche-like transport
  - Effect of 3D field on transport and MHD

- Disruption mitigation
  - Diagnostics for the Shattered Pellet Injection
  - Experiments on multiple SPIs

KSTAR is to address key physics and technical issues for ITER and DEMO

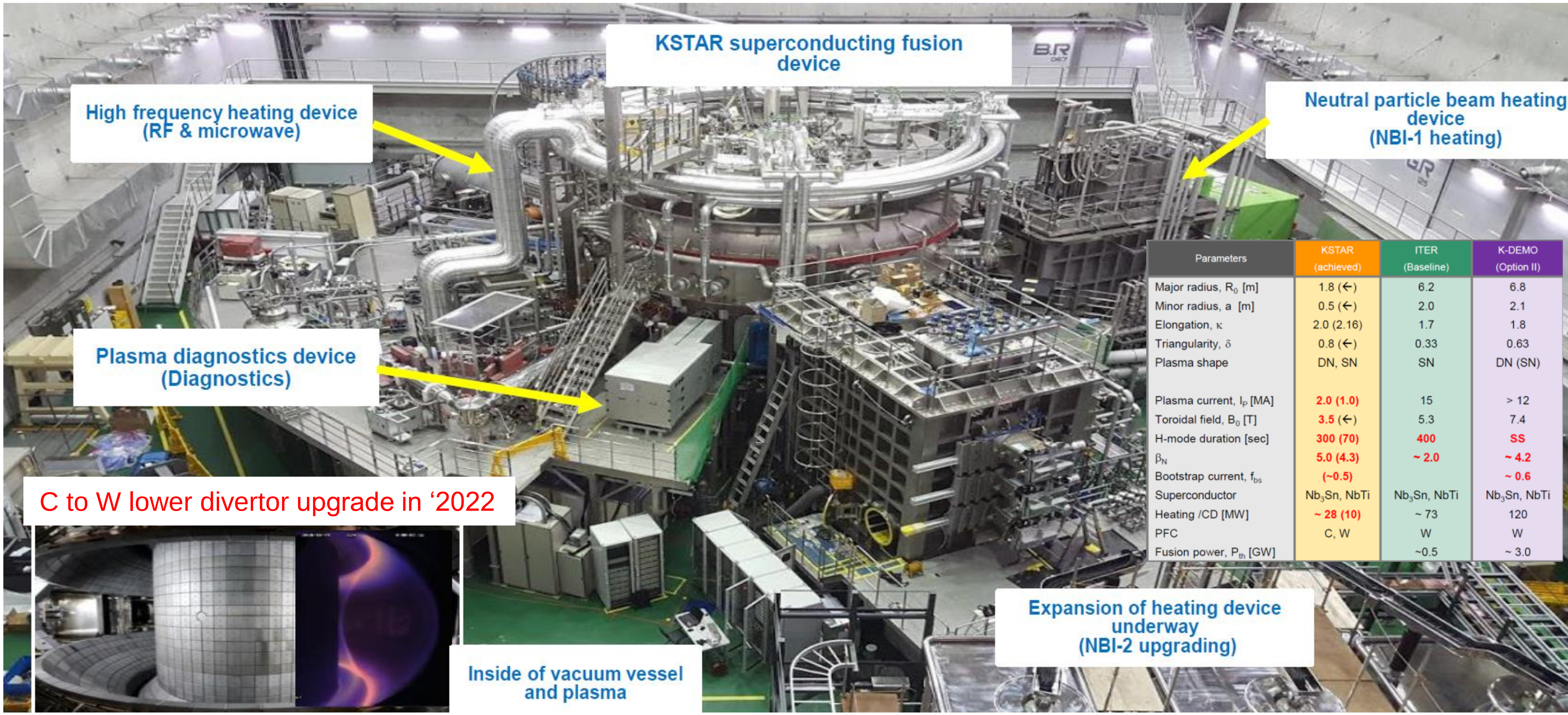

Parameters	KSTAR (achieved)	ITER (Baseline)	K-DEMO (Option II)
Major radius, R_0 [m]	1.8 (←)	6.2	6.8
Minor radius, a [m]	0.5 (←)	2.0	2.1
Elongation, κ	2.0 (2.16)	1.7	1.8
Triangularity, δ	0.8 (←)	0.33	0.63
Plasma shape	DN, SN	SN	DN (SN)
Plasma current, I_P [MA]	2.0 (1.0)	15	> 12
Toroidal field, B_0 [T]	3.5 (←)	5.3	7.4
H-mode duration [sec]	300 (70)	400	SS
β_N	5.0 (4.3)	~ 2.0	~ 4.2
Bootstrap current, f_{bs}	(~0.5)		~ 0.6
Superconductor	Nb_3Sn, NbTi	Nb_3Sn, NbTi	Nb_3Sn, NbTi
Heating /CD [MW]	~ 28 (10)	~ 73	120
PFC	C, W	W	W
Fusion power, P_{th} [GW]		~0.5	~ 3.0

Overall performances in various operating scenarios

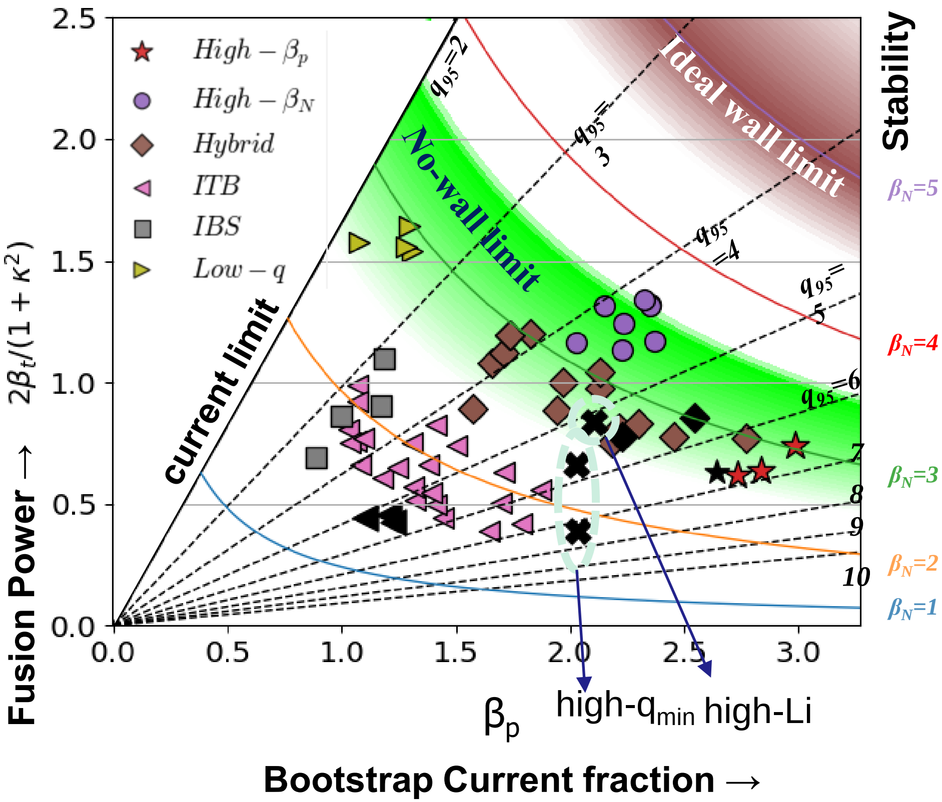

High Ip plasma operation

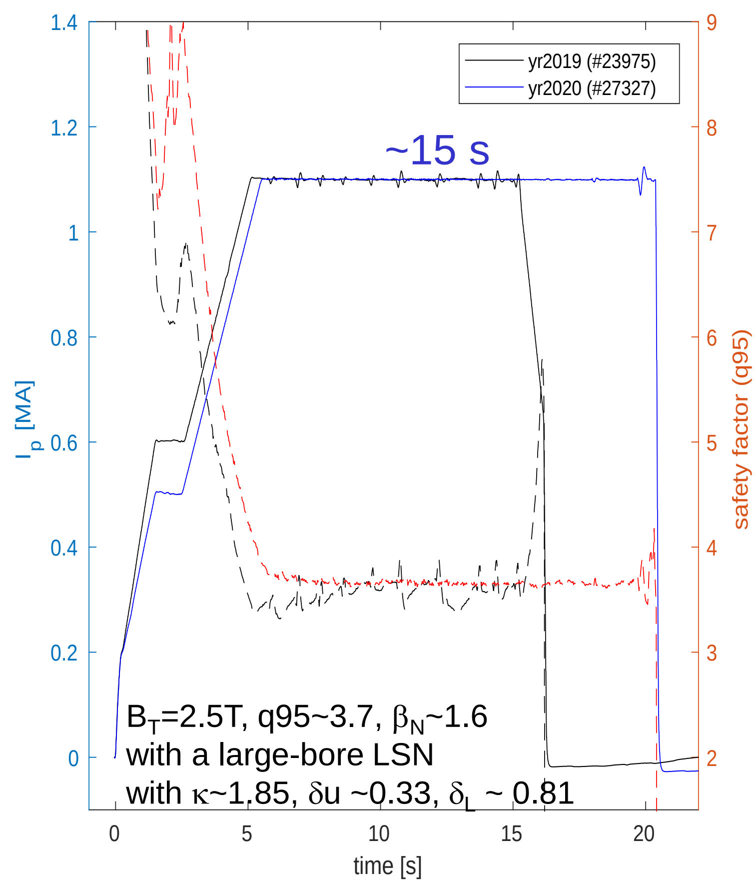

Extension of operation regime continues with new controls (symmetry control, ECCD)

Improved Access to High q_{min} (>2) for High β_N, Steady-State Scenario

- Access to high q_{min}
  - Early shaping
  - Early Heating & H-mode transition
- Slow β_N ramp during target formation
  - Minimize injection power and avoid MHD
  - Maintain high q_{min}
- Strong dependency of confinement on q_{min}
  - Improved confinement for broader current profile

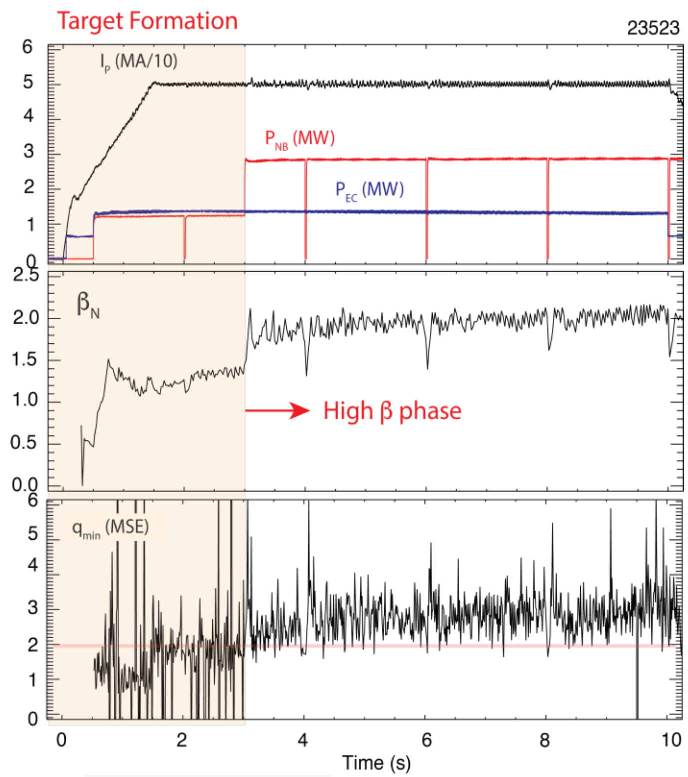

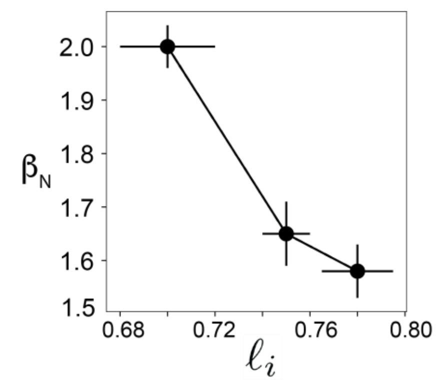

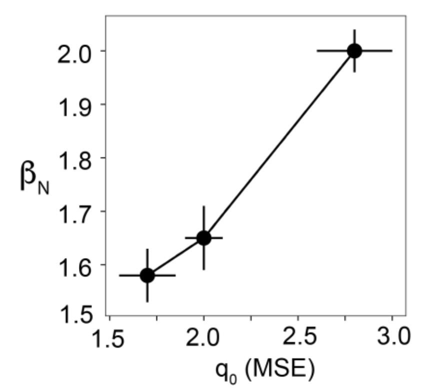

J. M. Park, ORNL

High li Scenario Achieves $\beta_N \approx 3$, $V_{Loop} < 0$ at $q_{95} = 5$ but Transiently

- High performance, low $q_{min} \approx 1$ scenario
  - Ohmic target formation and rapid β_N ramp at the highest li
  - Efficient on-axis CD (central ECCD + NB)
  - Maintain stability at high β_N w/o wall stabilization
- Robust shape control during rapid β_N ramp achieved
  - Feed-forward shape control of X-point target
  - Eliminate long ELM period between H-mode transition and first ELM: Preheating + gas puff
- $\beta_N > 3$ sustained until n = 2 MHD onset
  - Confinement and mode onset time sensitive to Ip (or q_{95})

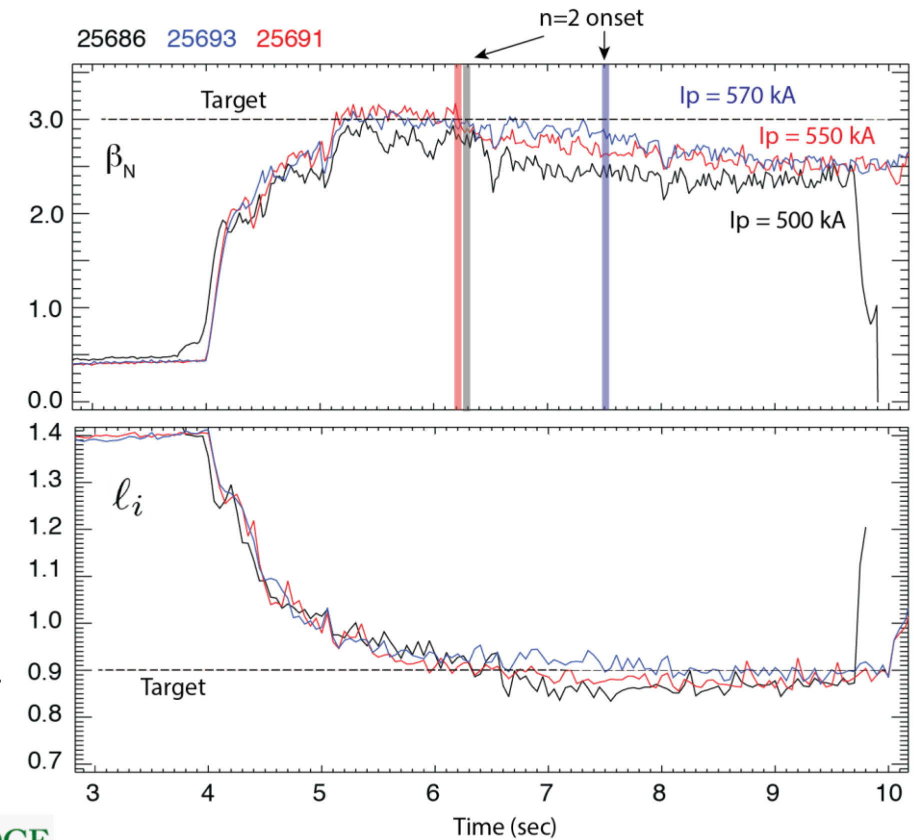

J. M. Park, ORNL

Transition to Hybrid mode by magnetic balance control

- In 2019-2020 experiments, transition from H- to hybrid mode was observed via dRsep control (-1.65cm → 0cm).
- #25460
  - β_n = 2.0 → 2.7, V_{loop} = 0.2 → 0.08 V
  - **dRsep from -1.65 cm → 0** (DN in 8.7-10 s)
- Hypothesis for the mechanism of transition

SEOUL NATIONAL UNIVERSITY

Y. S. NA, SNU

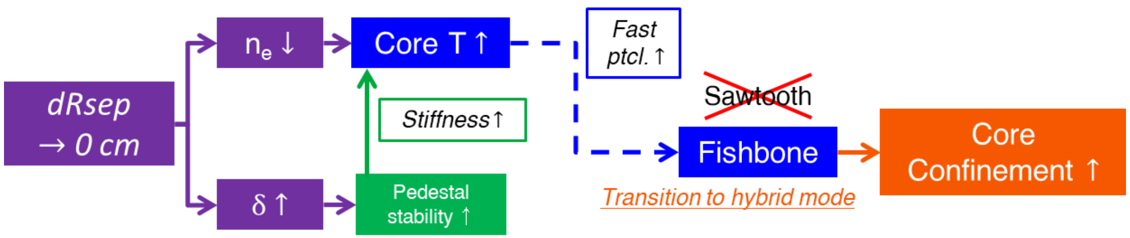

T_i profile [keV] (fitted)

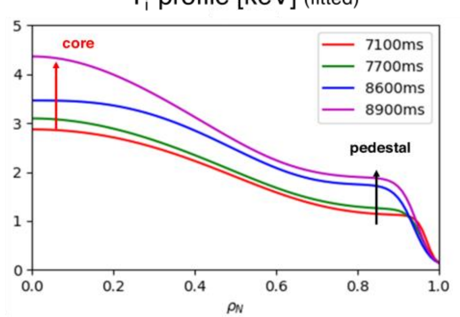

PBM stability boundary

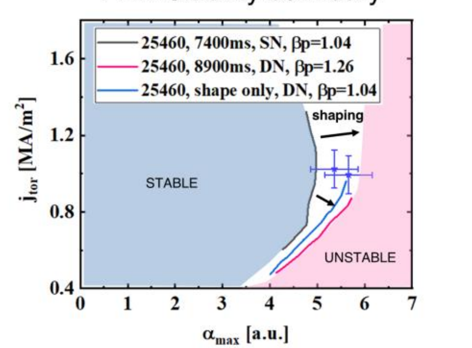

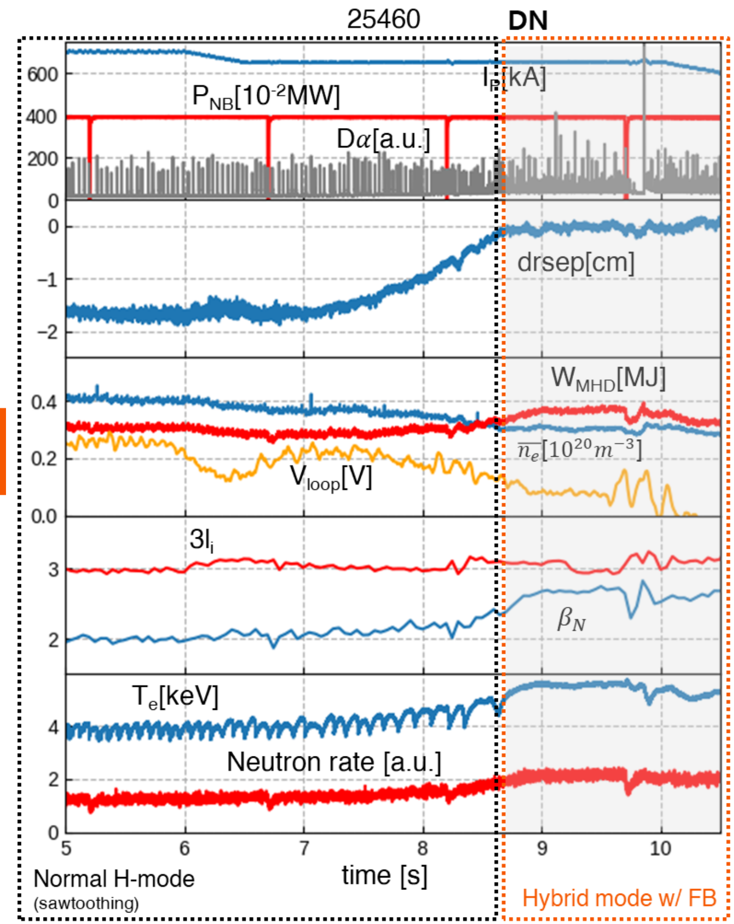

Long pulse sustainment(~30s) of Hybrid scenario

- #25530
  - Flattop sustained for **~30 s**
  - I_P = 0.6 MA, P_{total} = 5.04 MW
  - V_{loop} = 0.06−0.07 V, l_i ~1.02
  - Te constant, ne and Ti ↘, l_i ↗

SEOUL NATIONAL UNIVERSITY

Y. S. NA, SNU

- The performance was gradually degraded with $\beta_N = 2.6 \rightarrow 2.25$, mainly due to density and ion temperature drop.

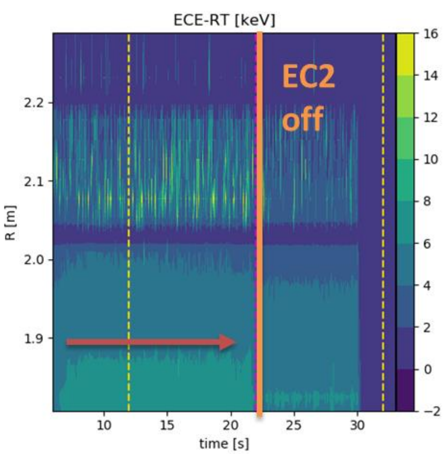

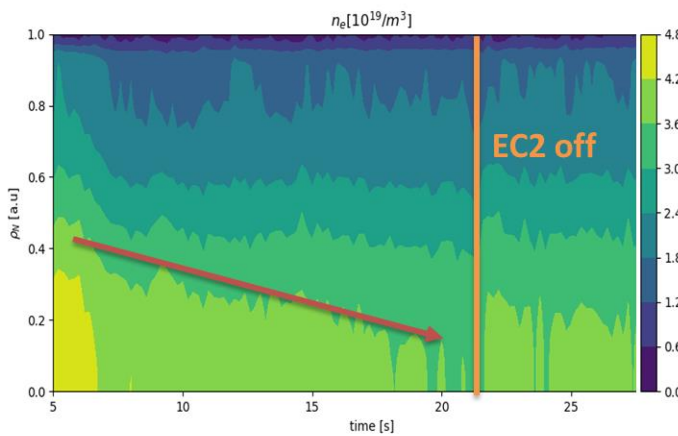

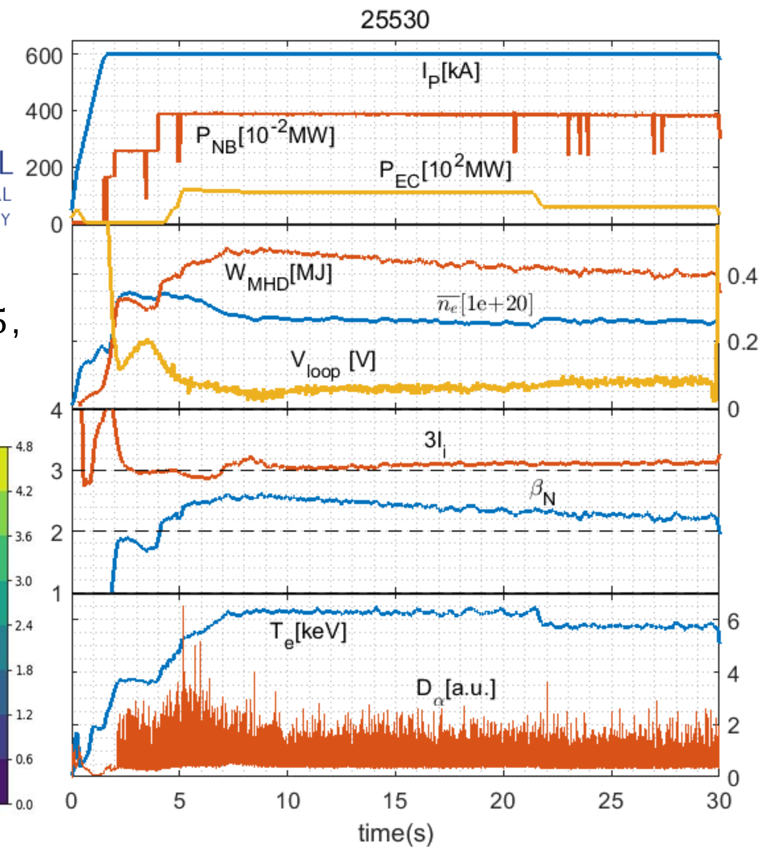

Recent high Ti discharge in diverted L-mode edge

- **Recently, KSTAR achieved stable diverted high T_i discharge (#25477) with L mode edge for ~ 20 s**
  - Ip = 0.6 MA
  - Bt = 1.8 T
  - q95 ~4.3
  - β_N~2.2
  - H_{89L} ~ 2.3
  - T_{i0} > 10 keV

- **Almost fully non-inductive current drive** with Loop voltage ~0.01 V
- There are n=1 energetic particle modes without sawtooth

Mirnov coil signal's Spectrogram (#25477)

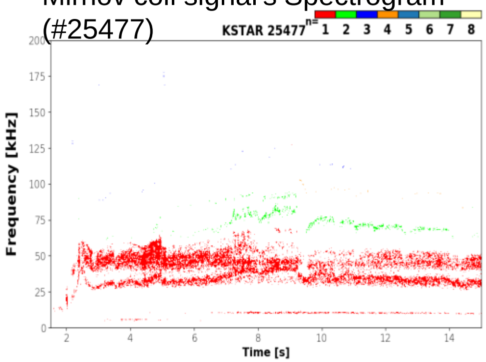

Ion Temperature (CES)

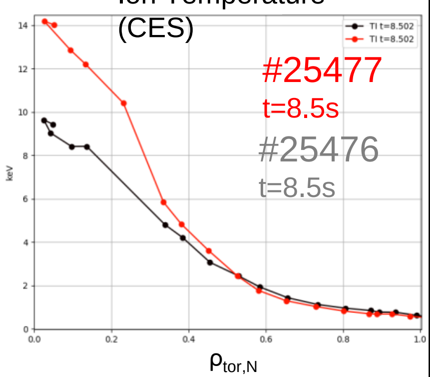

KSTAR #25860 (2020/10/16), Bt=1.8T

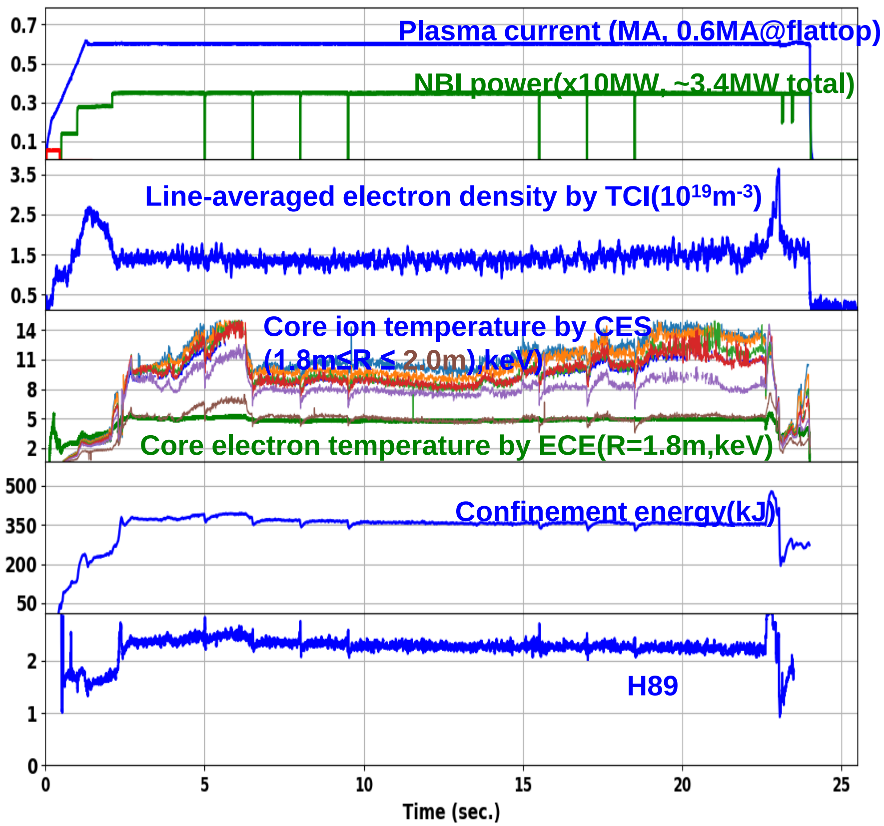

RMP-driven, ELM suppressions in KSTAR show a rather scattered dependence of pedestal density and collisionality

Empirically, low n_e and ν* plasmas are preferred for RMP-driven, ELM-crash-suppression

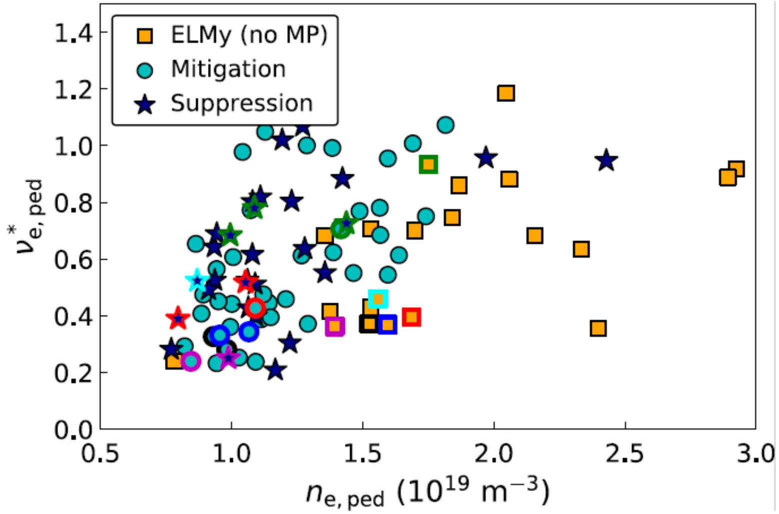

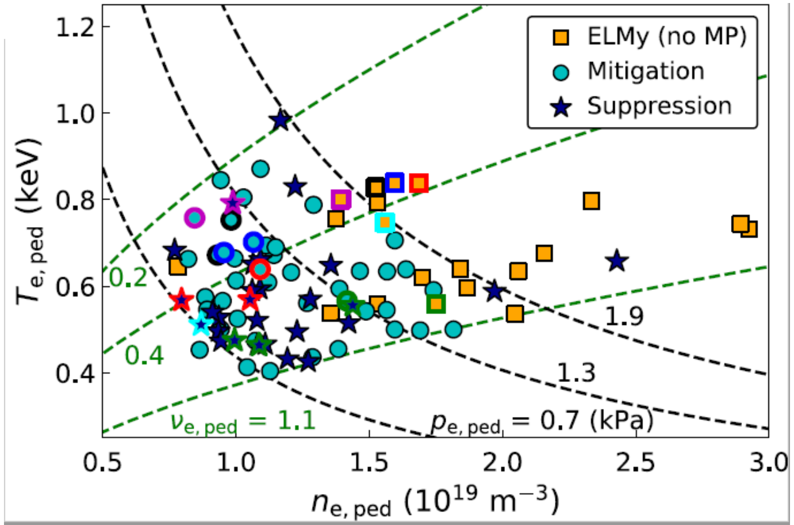

[M.W. Kim *et al*, to appear in Phys. Plasmas (2020)]

Nonetheless, no tendency is observed for RMP-driven, ELM-crash-suppression , according to the latest database in recent years (NOTE high n_e and ν* ELM suppression in KSTAR)

As RMP amplitude increases, the q_{95} window of n=1 RMP-driven, ELM suppression is expanded, consistent with theory

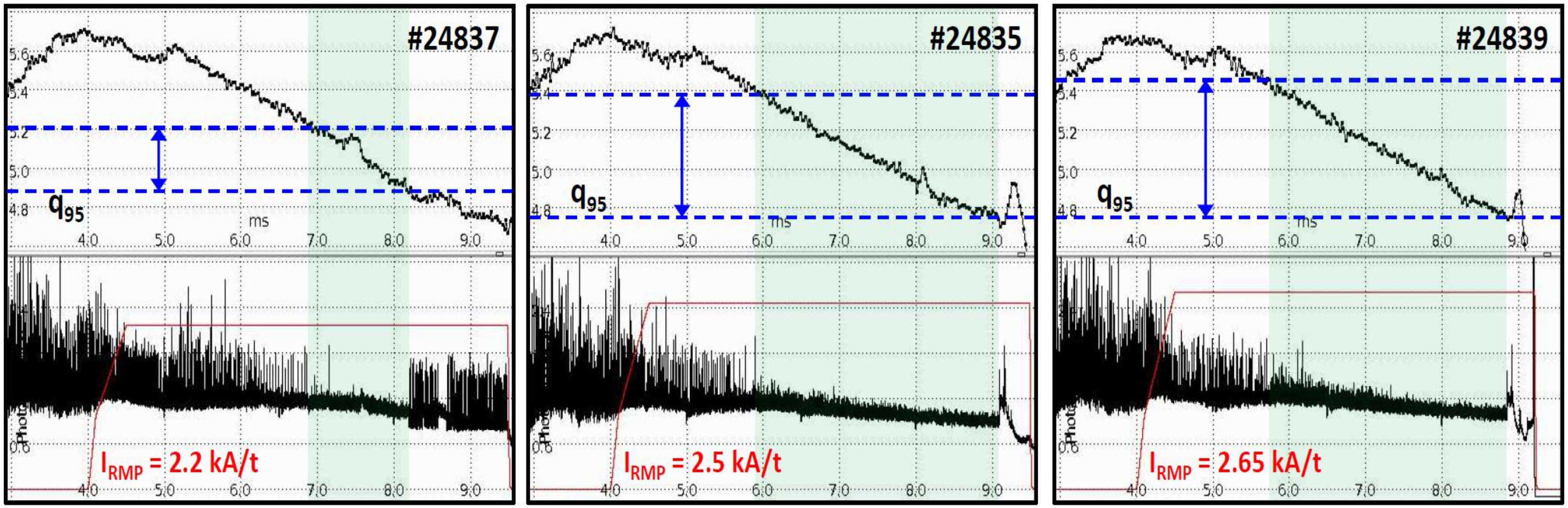

Once a large amplitude of RMP is utilized (without mode-locking), a wider range of q_{95} has been seen with RMP-driven, ELM-crash-suppression

[Y.M. Jeon, to be published (2020)]

-Predicted by TM1 [Q. Hu (PPPL)] PPPL PRINCETON PLASMA PHYSICS LABORATORY

KSTAR

High density plasma was successfully detached without impurity seeding, and has been sustained at modest level of RMP

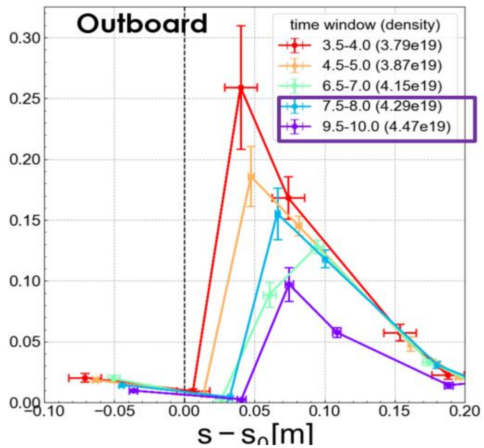

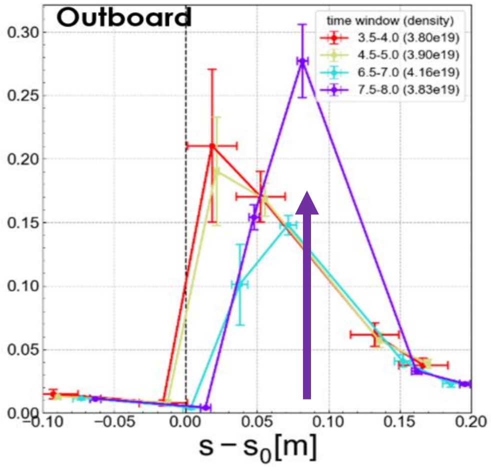

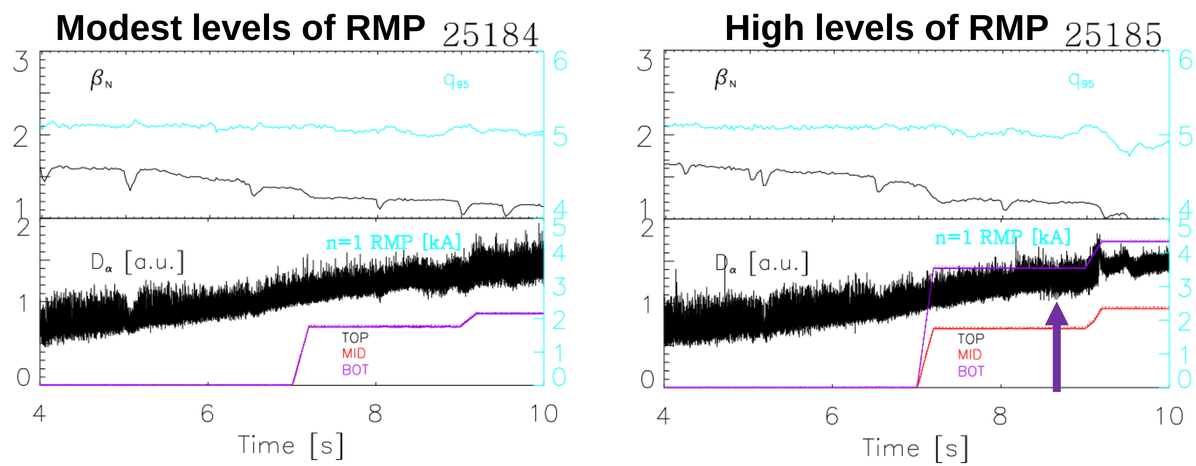

[Y. In, H.H. Lee, J.H. Hwang *et al*, to be published (2020)]

However, at high level of RMP, the plasma gets re-attached, along with noticeable density pump-out

Y. In, UNIST

As expected [Frerichs *et al*, PRL (2020)], substantial reduction of the divertor heat fluxes have been measured in detached plasmas, even resulting in very low level of signal-to-noise ratio on IR camera

Nonlinear RMP response contributes to the pedestal degradation and increased heat flux during RMP ELM control

- **Nonlinear 3D MHD modeling on KSTAR shows that RMP drives kink-tearing response, influencing the pedestal transport and divertor heat flux.**
  - Degraded pedestal leads to increased background heat flux
- **Plasma response can be changed by the MHD mode coupling with ELM.**
  - Enhanced stochastic layer and pedestal transport by RMP-ELM coupling
  - Importance of mode coupling to fully describe the RMP-driven plasma response

JOREK, KSTAR #18594 n=2 (Poincare plot)

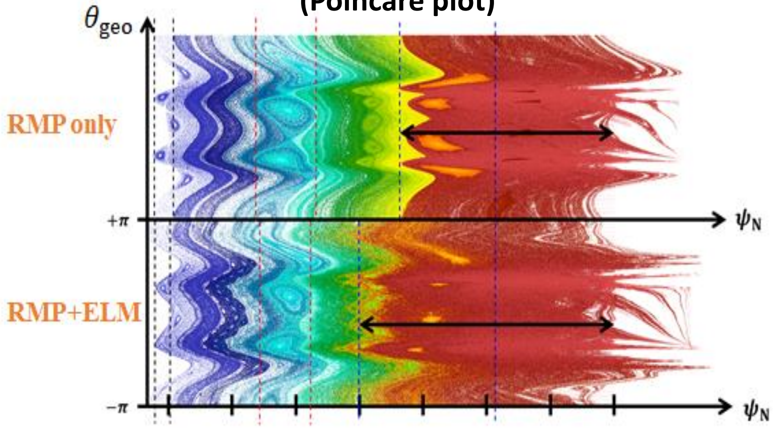

JOREK, KSTAR #18594 n=2 (Pedestal degradation plot)

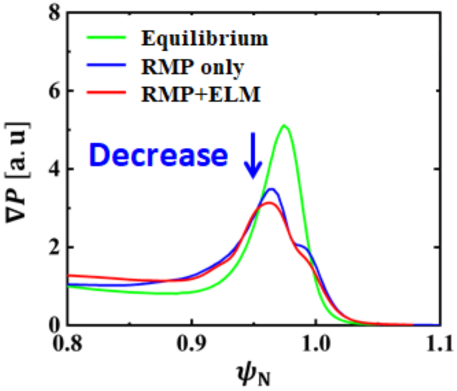

JOREK, Divertor heat flux (Lower LFS)

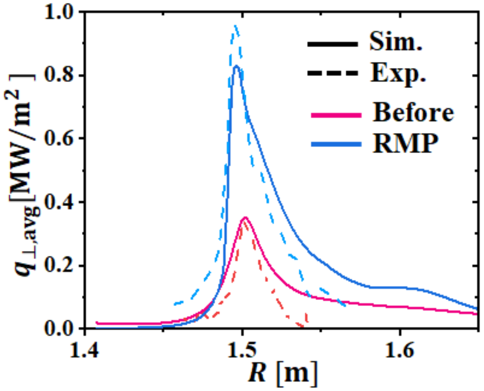

RMP-driven ELM suppression is successfully reproduced with RMP+ELM+NTV integrated simulation

- **Integrated MHD modeling shows that RMP (n=1,2) can suppress ELM crashes**
  - Full suppression of ELM burst
  - Significant reduction of bursty heat flux (But, 2 times larger background heat flux)
- **NOTE that ELM crash suppression by RMP is the consequence of RMP response**
  - Degraded pedestal gradient (Reduced instability source)
  - RMP-ELM mode coupling (Reduced bursty behavior ELM in nonlinear phase).

JOREK, ELM-crash suppression
(n=1 #21072, n=2 #18594)

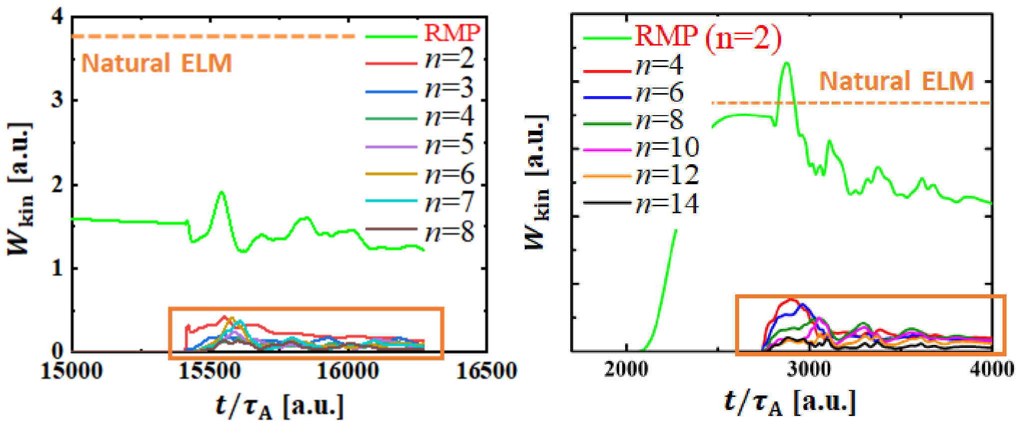

JOREK, n=1 #21072
(Disappeared ELMy heat flux)

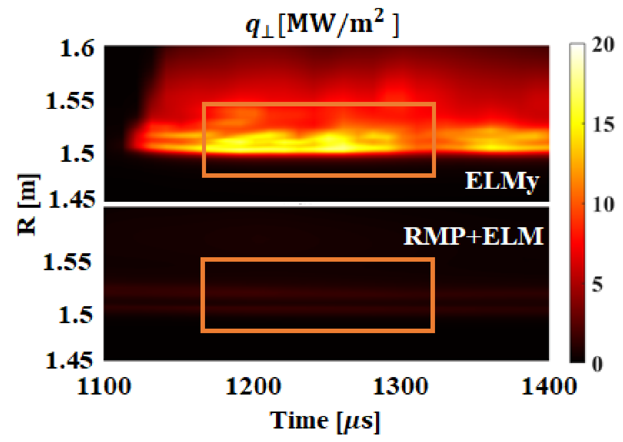

Adaptive ELM control successfully optimizes the RMP level, maximizing the confinement recovery while maintaining ELM suppression

- **ELM suppression with adaptive ELM control**
  - ✓ Successful ELM suppression and confinement optimization by adaptive control.
  - ✓ Recovered confinement up to 60% ($H_{98} = 0.7 \rightarrow 0.9$).
  - ✓ Mainly due to stably/quickly converged RMP level.
  - ✓ Converged within 4 iterations, ~5 s.

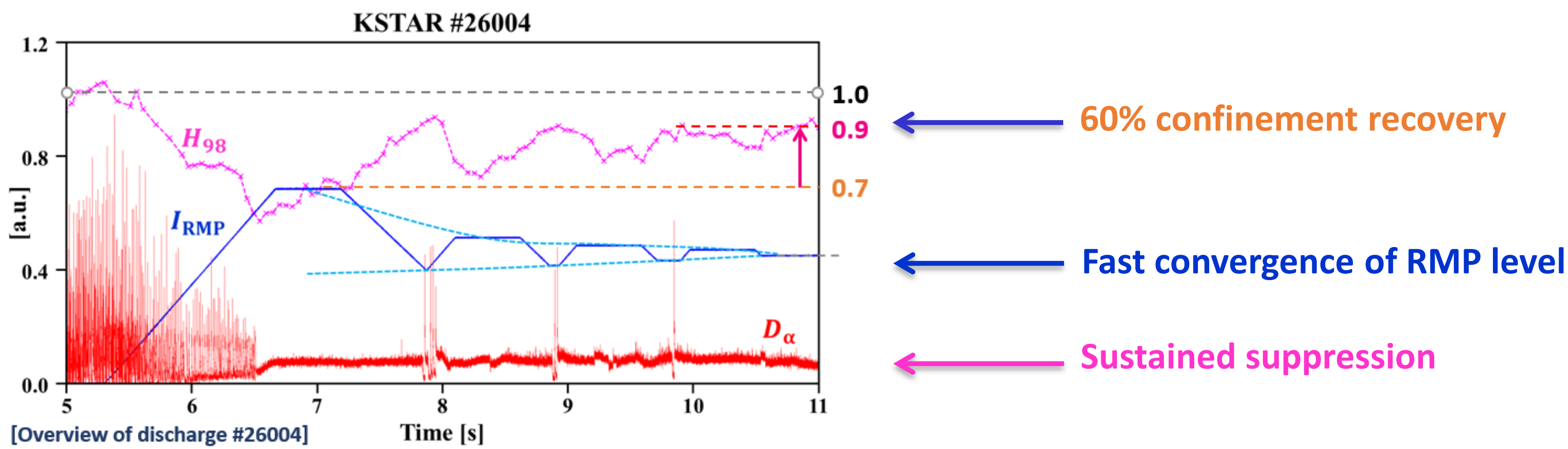

Decreasing the RMP amplitude until the loss of ELM-crash-suppres sion (2.5 kA down to 1.7 kA), and then reversing the the RMP chang e for ELM-crash-suppression

[R. Shousha and S.K. Kim, to be published (2020)]

Evidence of up/down asymmetric coupling difference for RMP ELM suppression, showing a meritorious use of Mid/Bot, instead of Top/Mid

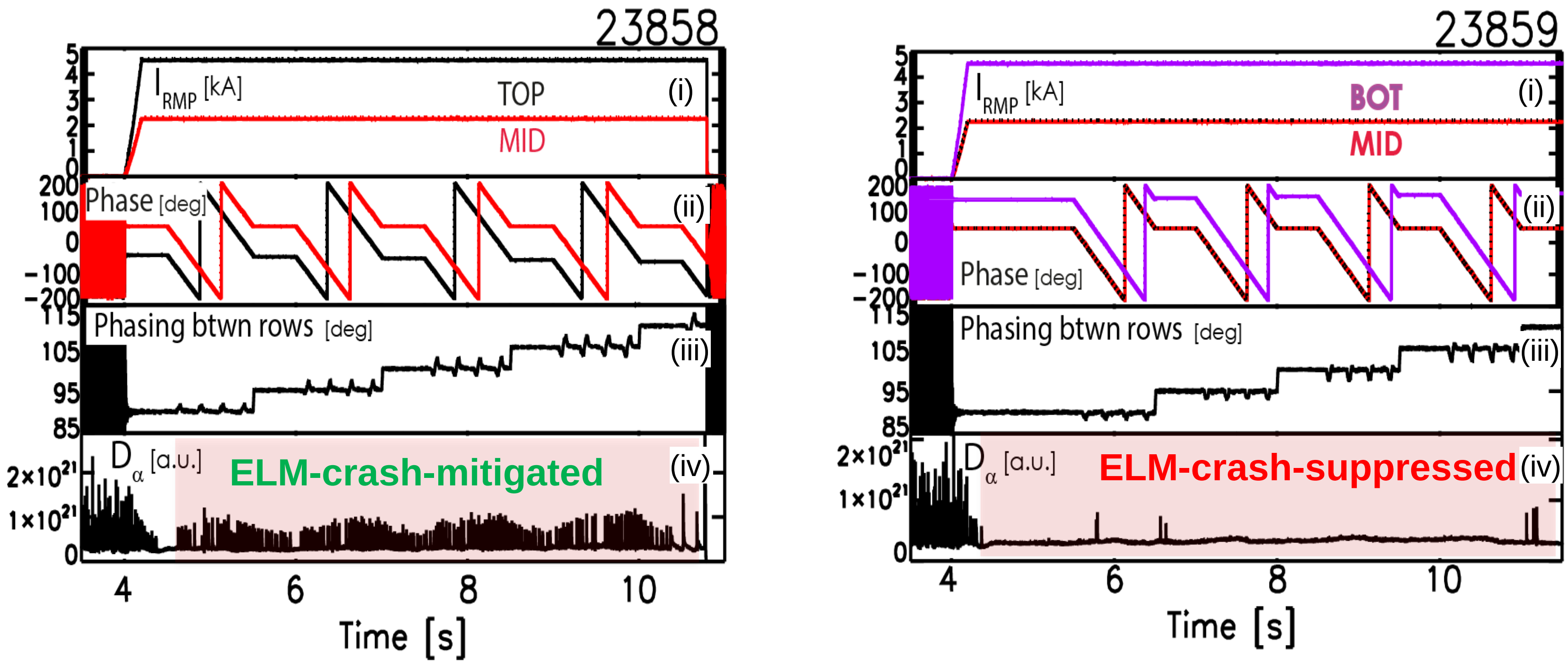

- **Potentially critical information for ITER RMP operation**
- **Much more reduced level of Bottom row was found to be sufficient, suggesting a weak coupling of top-row in 3-row IMCs**

Machine Learning (ML)-based RMP ELM control can successfully suppress first ELM right after L-H transition

- Real-time ML algorithm was shown to be working properly: classification + applying RMP
- First ELM was successfully suppressed by applying RMP during ELM-free period right after the L-H transition
- ML-based method has positive effects on sustaining high-beta plasmas during the whole discharge period

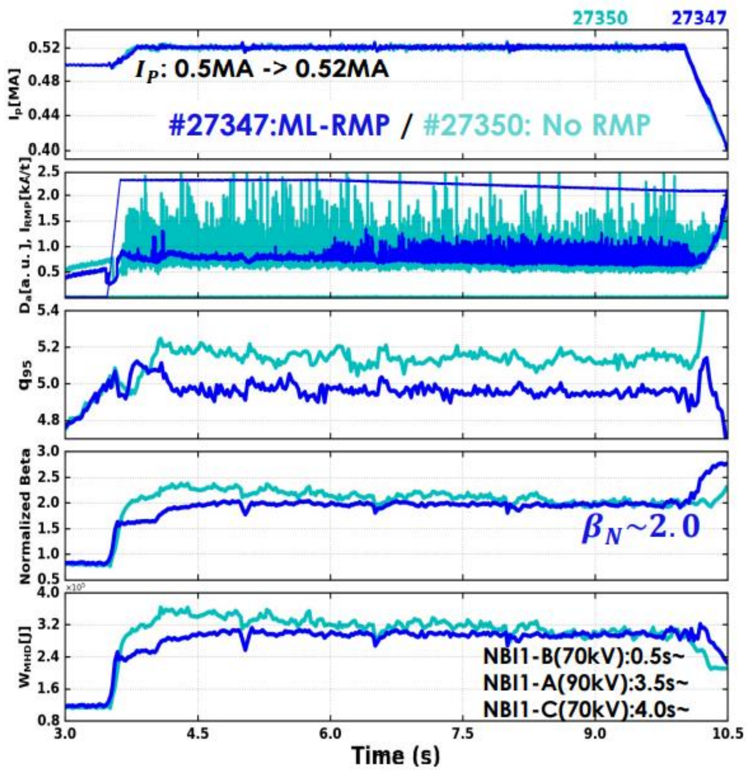

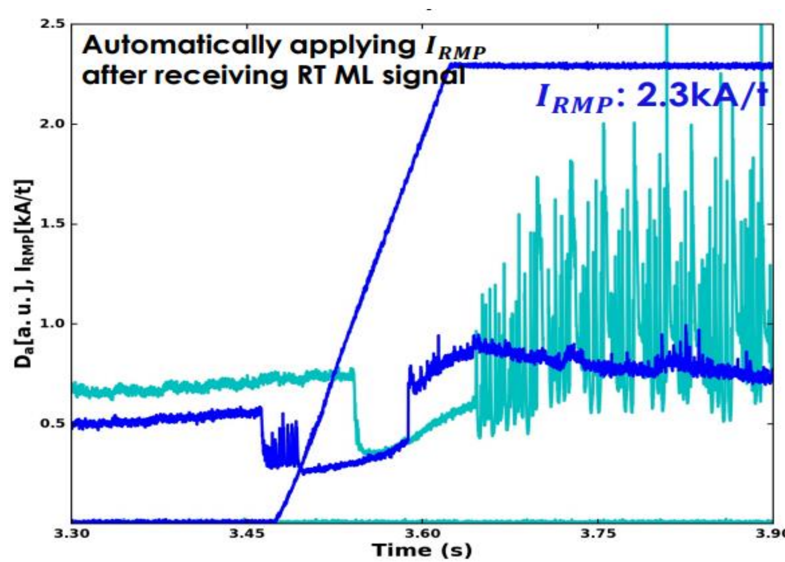

- First ELM suppression success
  - ✓ Adjust $q_{95} \sim 5.0$
  - ✓ Increase I_{RMP} : 2.1 → 2.3kA/t

KSTAR

KSTAR is successfully testing a comprehensive error field correction scheme using a concept of QSMP

Quasi-symmetric magnetic perturbation (QSMP) in a tokamak: A 3D field that can induce minimum neoclassical 3D transport, compared to NRMP or RMP, as successfully tested in KSTAR and DIII-D

Implies: Error field can be modified towards QSMP in correction, to minimize both resonant or non-resonant effects – more comprehensive or alternative scheme in error field correction problems in tokamaks

KSTAR QSMP configuration, with large dB but minimum impact o n 3D transport

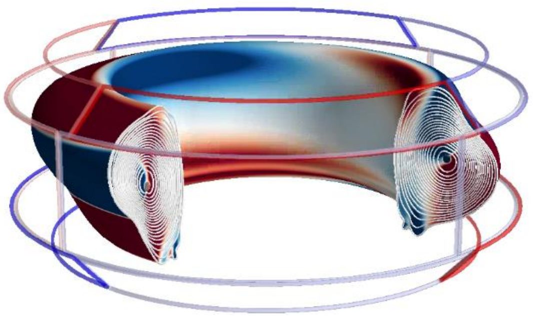

[1] J.-K. Park et al., PRL under review (2020)

NTV prediction for QSMP, NRMP, RMP

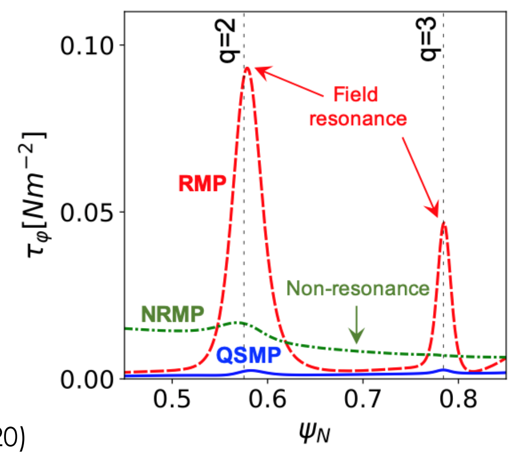

Experimental comparisons

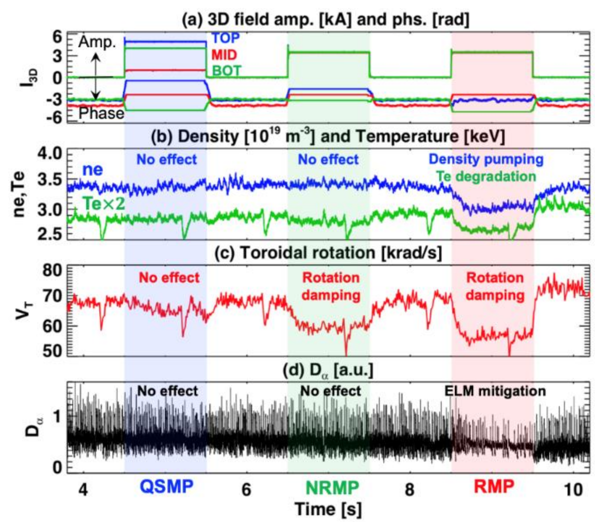

J. –K Park, PPPL

High-k scattering diagnostics provides key insight on relation between turbulence and MHD stability

- Transition of coherent mode to QCM

W. Lee, accepted in NF & ibid (MF1-O11)

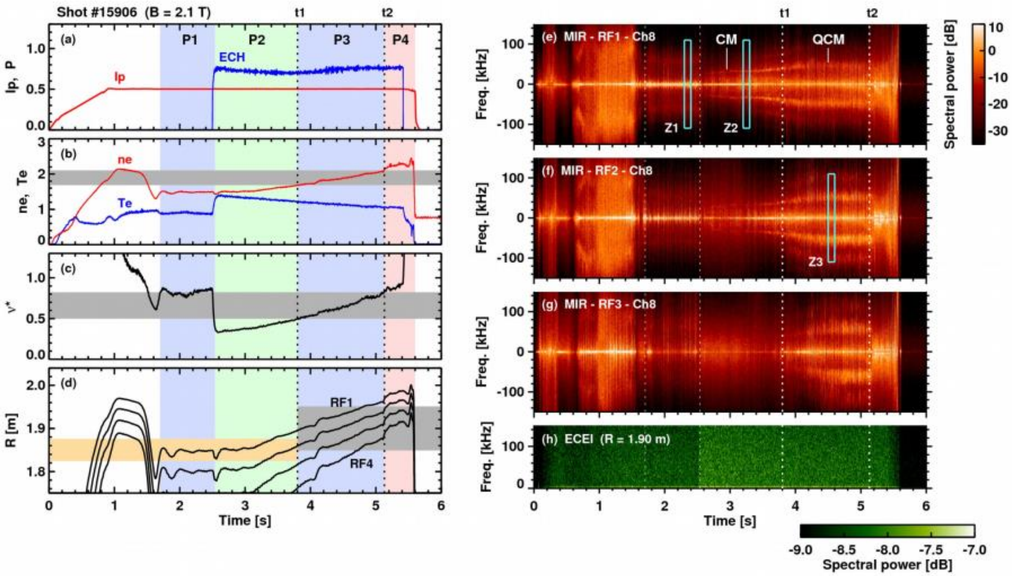

Collisional wavenumber broadening of coherent mode is a mechanism of the quasi-coherent spectrum

- High-k density fluctuations are now routinely measured by CSS diagnostics *W. Lee, submitted to PPCF*

Turbulence suppression after LH transition

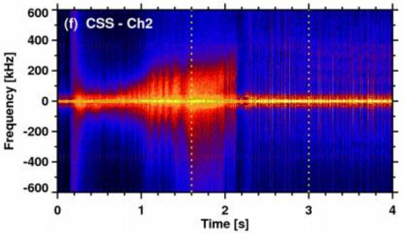

Turbulence increase with reduced ELM size

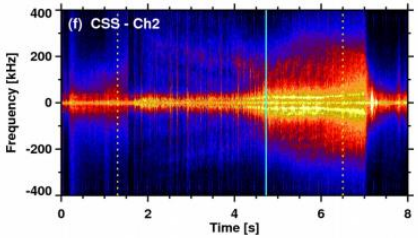

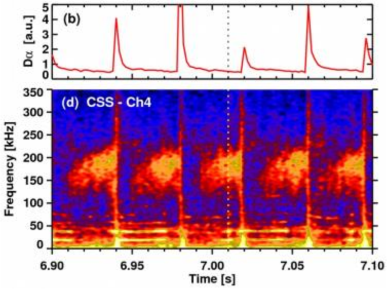

Gradual increase of turbulence before ELM crashes

Nonlinear energy transfer provides key insight on relation between turbulence and MHD stability

- Nonlinear three-wave coupling and energy transfer from ELM to broadband density turbulence during the ELM crash event *J. Kim, NF 60, 124002 (2020)*

Squared-bicoherence

$$b^2(f_1, f_2) = \frac{|\langle F_n(f_1)F_n(f_2)F_n^*(f_1+f_2)\rangle|^2}{\langle |F_n(f_1)F_n(f_2)|^2\rangle\langle |F_n^*(f_1+f_2)|^2\rangle}$$

Strong bicoherence shows the nonlinear coupling between ELM and turbulence

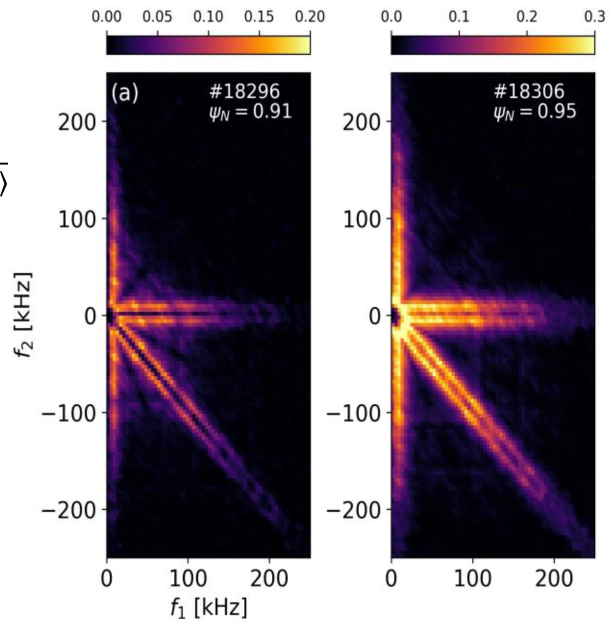

Analysis of quadratic energy transfer rate [Ritz PFB 1989, de Wit JGRA 1999] revealed the direction of the energy transfer

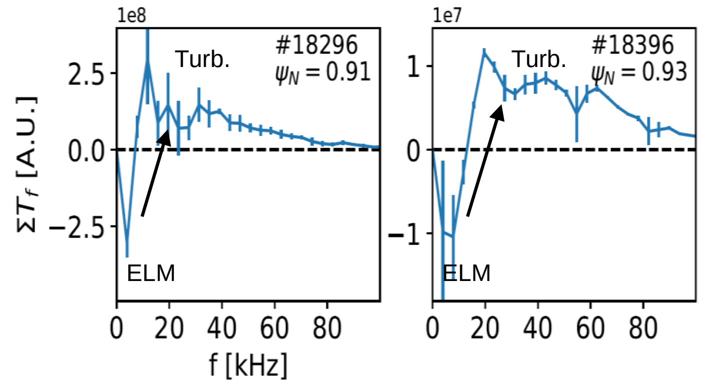

Turbulence spreading around magnetic island : Rapid heat transport and reconnection inside island

- Complex effects of the Te turbulence on the magnetic island evolution

M. Choi, submitted to Nature Comm.

Spontaneous Te peaking inside the island due to the turbulence spreading has a stabilizing effect

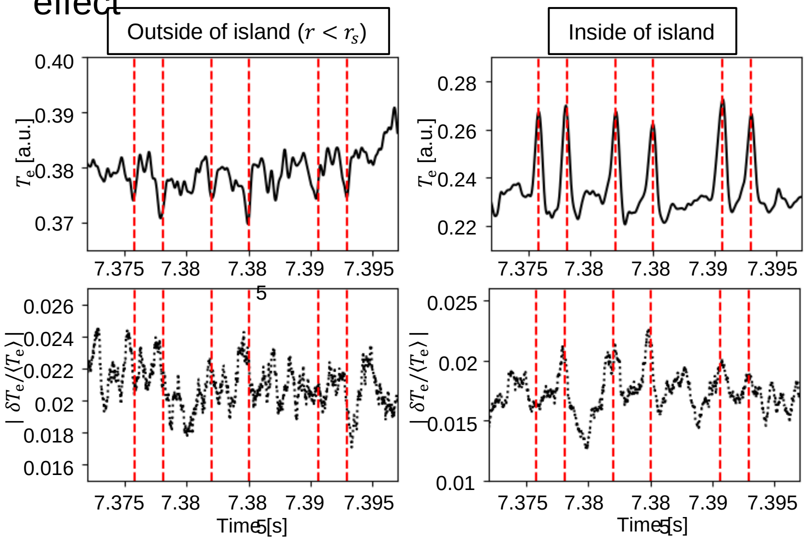

Turbulence enhancement at the reconnection site (X-point of the island) leads to the further reconnection and field stochastization, i.e. minor disruption.

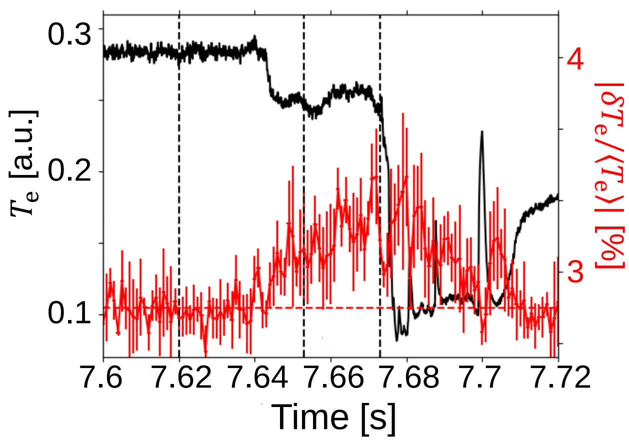

KSTAR

ExB shear regulates Avalanche-like transport in L-mode (1)

- Avalanche-like heat transport events and their regulation by ExB shear flow layers in MHD quiescent KSTAR L-mode plasmas

M.J. Choi, NF 59, 086027 (2019) & ibid (F-I43)

Large events are indicated by dashed lines
Small events are highlighted grey

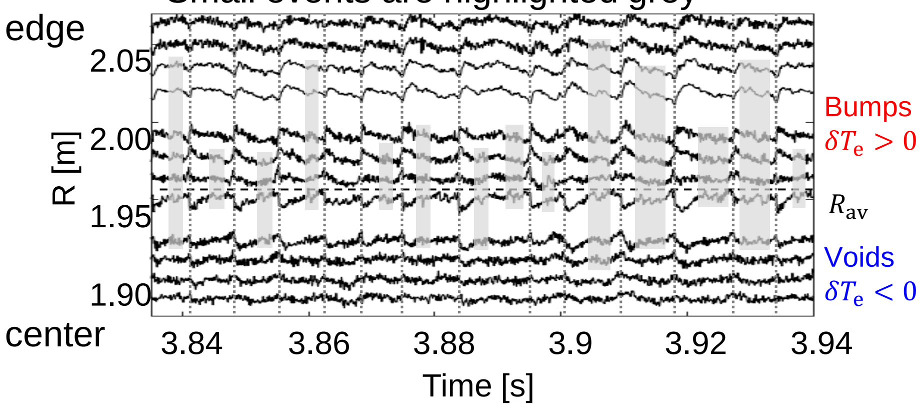

Te profile corrugation = shear flow layers

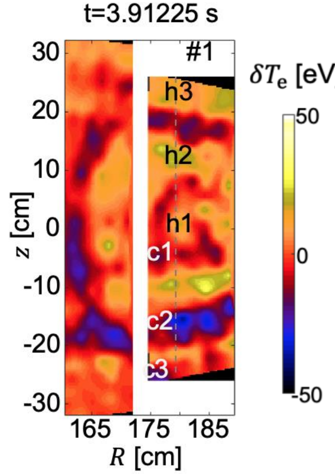

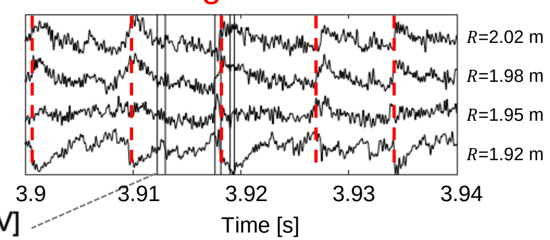

The vertical cut of δT_e

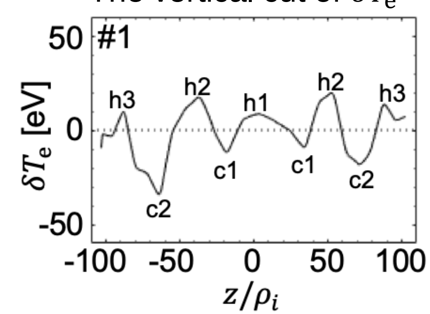

When shear layers exist, the size of the avalanche-like events is limited in the mesoscale ($\sim 45\rho_i$).
Large events occur after the shear layers are destroyed.

ExB shear regulates Avalanche-like transport in L-mode (2)

- Gyrokinetic simulation of KSTAR L-mode plasmas reproduces electron heat avalanches and zonal ExB shear flow layers *L. Qi, submitted to NF*

Similar power-law spectra of avalanche Te perturbations $|\delta T_e(f)|^2$: $S(f)\sim f^{-0.7}$

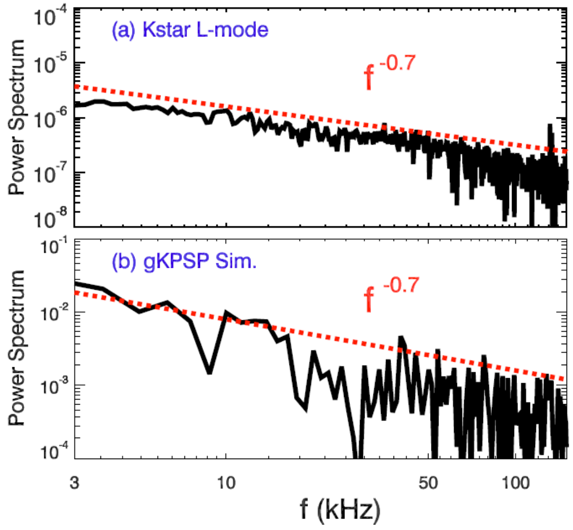

Quantitative agreement of the width of the profile corrugation

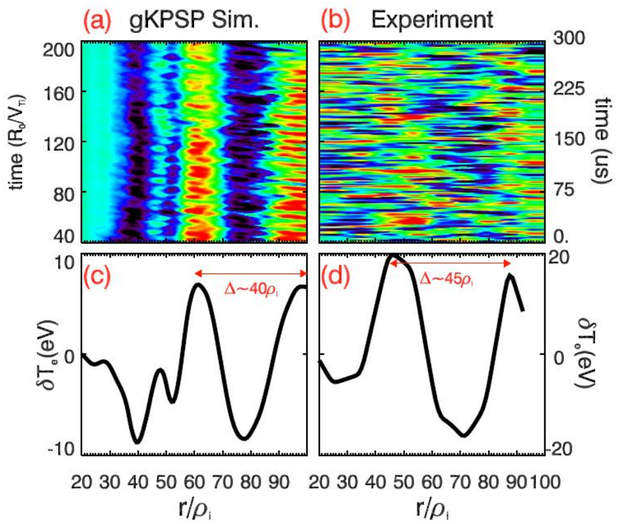

3D field effect on transport and Alfven Eigenmodes

- 3D magnetic breaking improved energy confinement

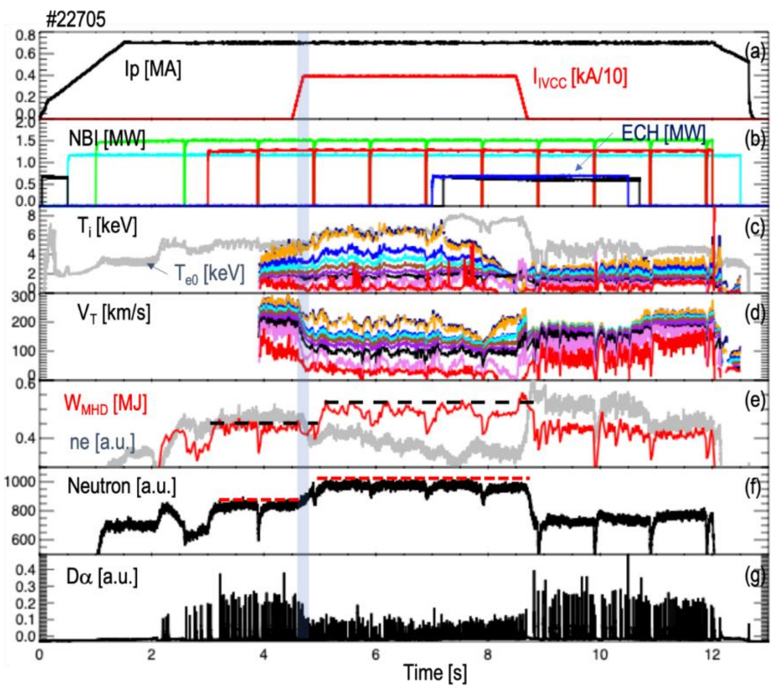

- TAEs are destabilized by 3D magnetic breaking

K. Kim, NF 60, 126012 (2020)

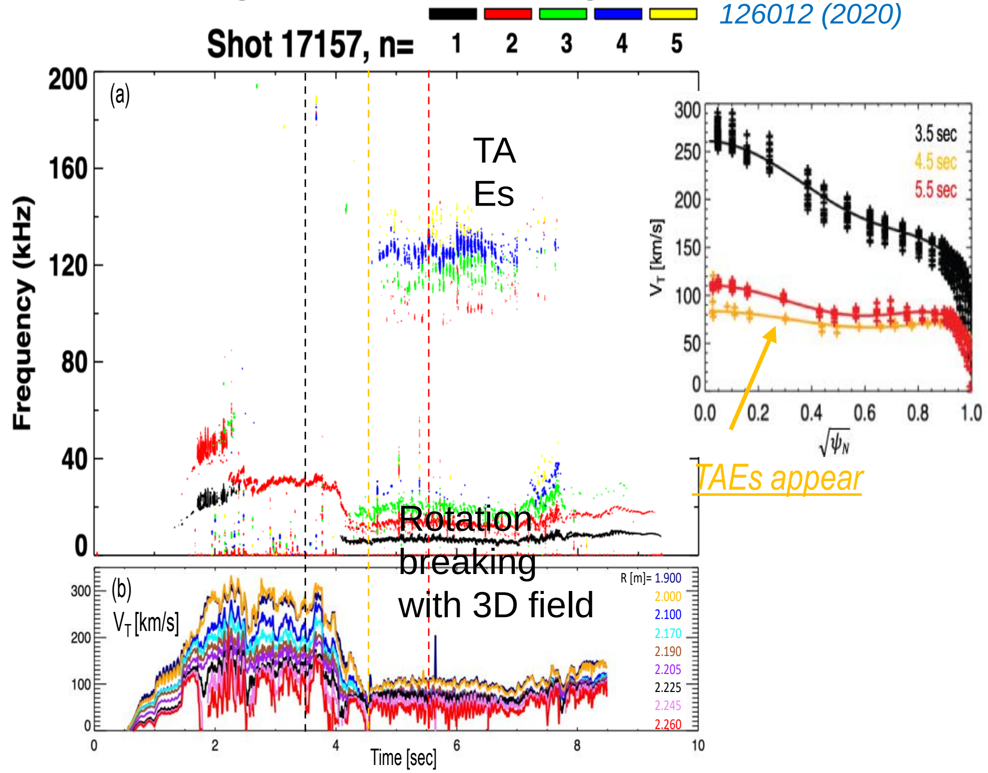

KSTAR dual SPI experiments demonstrated the feasibility of simultaneous multiple injection planned in ITER

- Two identical SPIs were installed in toroidally opposite locations in KSTAR in collaboration among IO, ORNL, and NFRI
- Low Z (D_2), high Z (Ne, Ar), and their mixture can be injected selectively.
- Three barrels in each SPI control the pellet size (i.e., amount of particles): 4.5 mm + 2x7.0 mm

  - KSTAR volume: 1.8 x π x $(0.45)^2$ x 2 x π x 3.14 x 1.8 ~ 12.9 m^3
  - 4.5 mm: D# =2.18×10^{21}, Ne# =3.83×10^{21}, Ar# =5.37×10^{21}
  - 7.0 mm: D# =8.77×10^{21}, Ne# =1.54×10^{22}, Ar# =2.16×10^{22}
  - 8.5 mm: D# =1.60×10^{22}, Ne# =2.82×10^{22}, Ar# =3.96×10^{22}

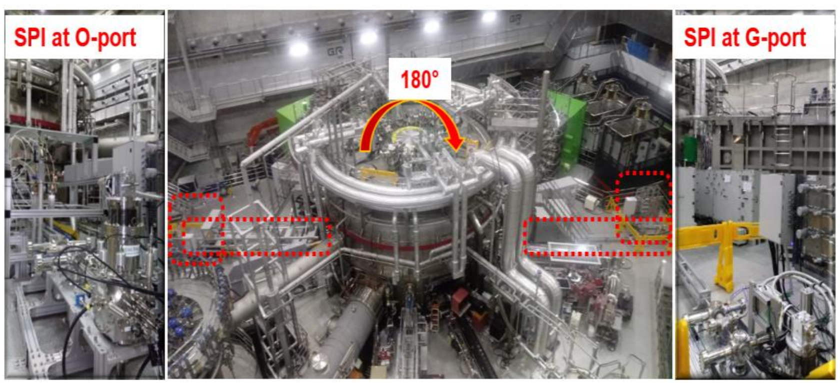

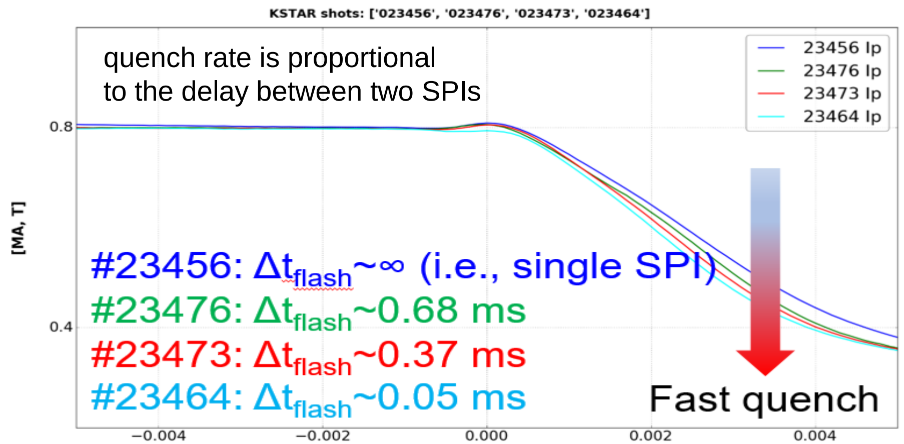

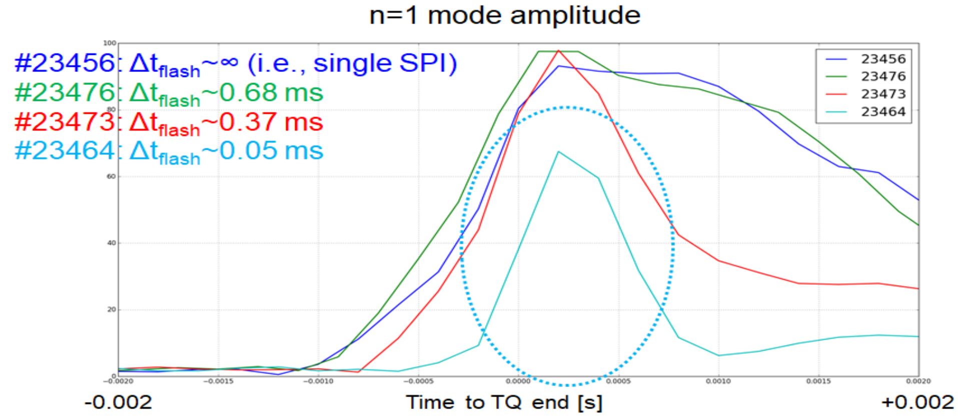

KSTAR dual SPI experiments demonstrated the feasibility of simultaneous multiple injection planned in ITER

- Two identical SPIs were installed in toroidally opposite locations in KSTAR in collaboration among IO, ORNL, and NFRI
- Low Z (D_2), high Z (Ne, Ar), and their mixture can be injected selectively.
- Three barrels in each SPI control the pellet size (i.e., amount of particles): 4.5 mm + 2x7.0 mm
  - KSTAR volume: 1.8 x π x $(0.45)^2$ x 2 x π x 3.14 x 1.8 ~ 12.9 m^3
  - 4.5 mm: D# =2.18×10^{21}, Ne# =3.83×10^{21}, Ar# =5.37×10^{21}
  - 7.0 mm: D# =8.77×10^{21}, Ne# =1.54×10^{22}, Ar# =2.16×10^{22}
  - 8.5 mm: D# =1.60×10^{22}, Ne# =2.82×10^{22}, Ar# =3.96×10^{22}

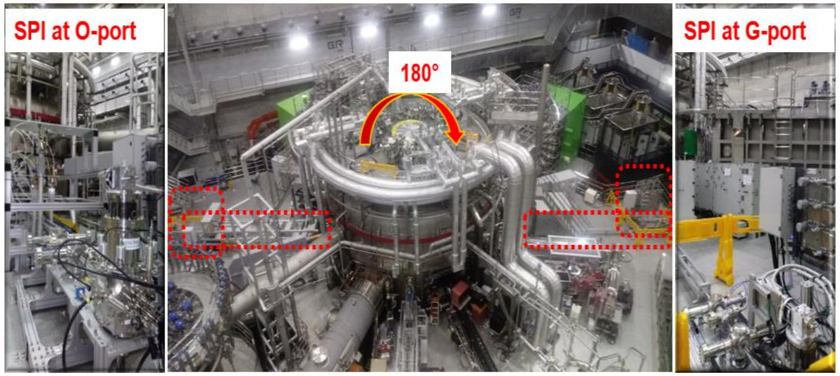

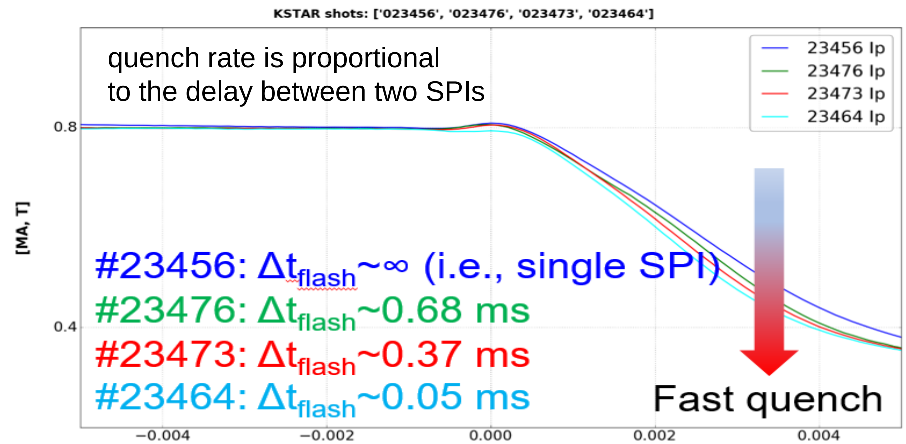

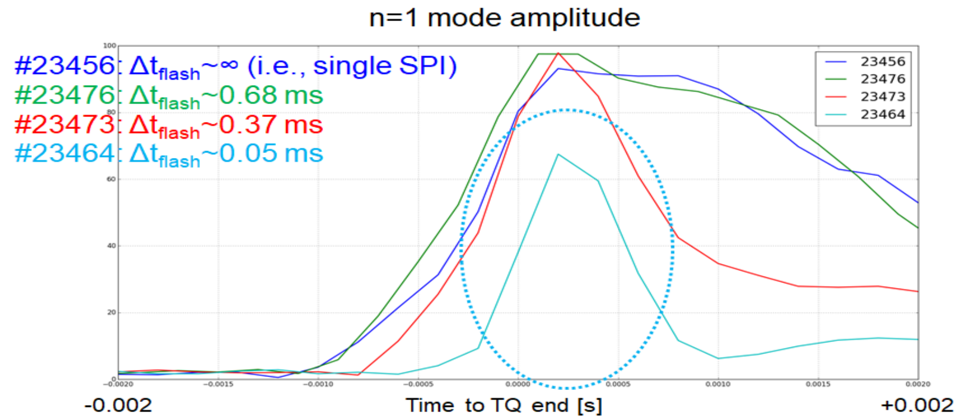

SUMMARY

- Enhanced performance in various operating regimes was obtained and machine parameters were expanded, including early diverting, sustainment of the centrally peaked high ion temperature mode, hybrid scenario, stationary high beta discharge and long-pulse H-modes
- Key issues for RMP ELM suppression has been further resolved focusing on the optimal poloidal spectrum, collisionality, and the real-time control capability for minimum performance degradation
- Cross-validation between the advanced diagnostics and the modeling provides new insight on the fundamental transport process including avalanche-like electron heat transport and QCM
- Providing unique demonstration on the performance of symmetric multiple Shattered Pellet Injections (SPIs) which is the main strategy of ITER for disruption mitigation